24. Shlomi, T., Berkman, O. and Ruppin, E., Regulatory on/off minimization of metabolic flux changes after genetic perturbations. *Proc. Natl. Acad. Sci., USA*, 2005, **102**, 7695–7700; doi: 10.1073/pnas.0406346102.
25. Lewis, N. E. *et al.*, Omic data from evolved *E. coli* are consistent with computed optimal growth from genome-scale models. *Mol. Syst. Biol*., 2010, **6**, 390; doi: 10.1038/msb.2010.47.
26. Lee, J. Y., Yang, K. S., Jang, S. A., Sung, B. H. and Kim, S. C., Engineering butanol-tolerance in *Escherichia coli* with artificial transcription factor libraries. *Biotechnol. Bioeng*., 2011, **108**, 742–749; doi: 10.1002/bit.22989.
27. Carbonell, P., Planson, A.-G. and Faulon, J.-L., In *Systems Metabolic Engineering Methods in Molecular Biology* (ed. Alper, H. S.), Humana Press, 2013, vol. 985, Ch. 9, pp. 149–173.
28. Planson, A. G., Carbonell, P., Paillard, E., Pollet, N. and Faulon, J. L., Compound toxicity screening and structure-activity relationship modeling in *Escherichia coli*. *Biotechnol. Bioeng*., 2012, **109**, 846–850; doi: 10.1002/bit.24356.
29. Reyes, L. H., Abdelaal, A. S. and Kao, K. C., Genetic determinants for *n*-butanol tolerance in evolved *Escherichia coli* mutants: cross adaptation and antagonistic pleiotropy between *n*-butanol and other stressors. *Appl. Environ. Microbiol*., 2013, **79**, 5313–5320.
30. Chin, W.-C., Lin, K.-H., Chang, J.-J. and Huang, C.-C., Improvement of *n*-butanol tolerance in *Escherichia coli* by membrane-targeted tilapia metallothionein. *Biotechnol. Biofuels*, 2013, **6**, 2–9.
31. Jin, H., Chen, L., Wang, J. and Zhang, W., Engineering biofuel tolerance in non-native producing microorganisms. *Biotechnol Adv*., 2014, **32**, 541–548; doi: 10.1016/j.biotechadv.2014.02.001.

ACKNOWLEDGEMENTS. We thank Pablo Carbonell, Sara Careia and Paulo Maia, for providing insight on RetroPath pathway predictions and OptFlux software applications respectively.

Received 13 May 2014; revised accepted 3 November 2014

# Morphometric analysis of Barren volcanic base and associated tectonic elements in the Andaman fore-arc sub-basin

**Saju Varghese* and G. Nagendran**

Marine and Coastal Survey Division, Geological Survey of India, Salt Lake, Kolkata 700 091, India

**Although many studies have been undertaken on the Barren Island, the undersea configuration of the Barren Island Volcano (BIV) and associated morphotectonic elements, the modification imparted on them by the recent flows and the morphology of these flows are still poorly known. The present study identified thick lava flows along the western and southwestern slopes of Barren Island, extending up to the base of the Invisible Bank. The feeding locales for these thick flows are numerous parasitic cones picked up in the 3D grid model generated by the multibeam echo sounder. Morphology of the Barren volcanic base is largely modified by recent eruptions as they not only reduced the steepness of the Barren Volcano along the western slope, but also extended the base of the Barren Volcano to the base of the Invisible Bank. Furthermore, the present study also brought out other morphotectonic elements surrounding the BIV, viz. Alcock seamount towards the southeast, Invisible Bank flanked by west Andaman Fault in the west and a newly identified submarine volcanic mount as part of the Andaman Volcanic Arc towards the south.**

**Keywords:** Alcock seamount, barren volcano, geomorphology, west Andaman Fault.

BARREN Island Volcano (BIV) is India's only active volcano lying about 135 km ENE of Port Blair within the exclusive economic zone (EEZ) of India. After 150 years of quiescence, it became active for five years from 1991 to 1995. BIV became active once again after a gap of 12 years on 28 May 2005. Being a part of the Neogene Inner Volcanic Arc (NIVA), BIV is located in the Andaman Sea which is a marginal sea on the western side of the Burmese continental mass marked with an oblique back-arc spreading centre[1,2]. Pal *et al.*[3] described the geology of the BIV with excellent descriptions, analyses and interpretations. This belt can be traced from the Central Molasse basin of Myanmar, through the Narcondam and BI into the structural trend of Sumangko rift zone, along the volcanic Barisan range axis of northern Sumatra[4] (Figure 1). Other important tectonic elements in the Andaman Sea are the Invisible Bank (IB), Diligent Fault (DF) and West Andaman Fault (WAF). IB is formed by thick lava flows overlain by sedimentary rocks of Middle Miocene extending to the east of Andaman and Nicobar Group of Islands, whereas DF and WAF form the western and eastern margin towards the northern part of the Andaman Sea respectively[2,5].

No attempts have been made so far to understand the undersea configuration of the BIV and associated morphotectonic elements. Furthermore, understanding of the extent of recent flows and their morphology is of paramount importance for understanding the evolution of the BIV. In addition, the disposition of other morphotectonic elements around the BIV is not yet understood in detail. With these objectives in mind, a full-fledged cruise SM-220 was mounted on-board *RV Samudra Manthan* to obtain the 3D sea-bed morphology of the Barren volcanic cone and associated geomorphic–tectonic features in the Andaman Sea. To bring out the undersea configuration of the Barren Island (BI) and surrounding morpho-tectonic elements, multibeam swath bathymetric survey was carried out in an area 5080 sq. km around Barren Island with

*For correspondence. (e-mail: saajuvarghese@gmail.com)

water depths 50–2350 m. The morphometry of the geomorphic and tectonic features like the 'Western Ridge', 'South-Western Ridge', WAF, Alcock seamount, submarine volcanic plug and the base of the BIV with inclined/parasitic vents has been brought out in detail by multibeam echo sounder survey (MBES; Figure 2 *b*).

A SeaBat™ 7150 (RESON) ultrahigh-resolution focused MBES system mounted on the hull of *RV Samudra Manthan* was used for the present survey. It operated at a frequency of 12 kHz for water depths greater than 1300 m and 24 kHz for water depths less than 1300 m. The projected arrays generate a single transmission with an along-track width of 1° and an across-track width of 150°. The transducer of the RESON SeaBat™ 7150 generates and transmits a sway of sound beams (256) down the water column, across the navigational tracks, whereas the transceiver unit of SeaBat™ 7150 receives beams reflected from the sea bed. In turn, the PDS 2000 software, installed in the acquisition unit, collates the bathymetric data with other relevant data input like positioning data, external clock and compass data. The DGPS MAX differential global positioning system interfaced with the acquisition unit was used to provide positioning data of ship to PDS 2000 software to collate the data with multibeam bathymetric data. An OCTANS™ surface gyrocompass and motion sensor was employed to provide true-heading, roll, pitch, yaw, heave, surge, sway, rate of turn and acceleration of the vessel, even in highly volatile environment. For the focus-forming process of the receiver beams as well as the conversion of measured return ping times into distances, a SVP™ 70 (RESON) sound velocity probe (SVP) was mounted close to the hydrophone. The SVP measures sound velocities in the range 1350–1600 m/s, with a resolution of 0.1 m/s and an accuracy of ± 0.25 m/s. The bathymetric data from RESON SeaBat™ 7150 were processed using PDS 2000. The bad depths (i.e. outliers) in the georeferenced multibeam original (raw) data were detected rationally and cleaned manually on PDS 2000 to prepare an unbiased seabed topography[6]. Using these manually edited data, 3D grid model of topographic surfaces was developed with pixel size 75 m. The survey layout consisted of long east–west traverses of 13 lines, north–south traverses of 30 lines, 32 cross lines and 6 straight lines with 4 circular traverses. Detailed profiles from the results are shown in Figure 3 *a*–*c*.

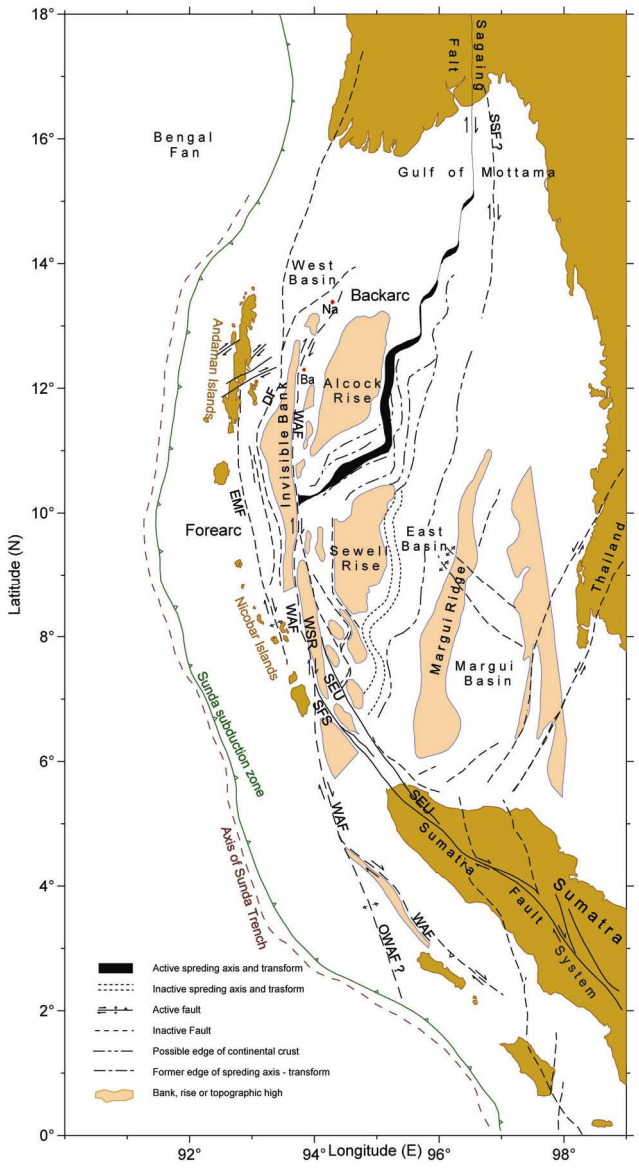


**Figure 1.** Tectonic map of the Andaman Sea with the location of Barren Island.

The present study shows that the base of BIV lies between 1876 m and 2363 m water depth. It has a maximum length of 33.7 km along N–S direction and minimum length of 27 km NW–SE direction (Figure 3 *a* and *c*). Profile studies of the bathymetric map (Figure 4) generated revealed that the circumference of the base of BIV on the seafloor varies from 87.79 to 112.85 km and the slopes are steeper in NNE and SSE directions. A few small, submerged elevated mounts scaling from 30 to 750 m high, are seen on the western, southwestern and southern submarine slope of the BIV (Figures 2 *b* and 5 *c*, *d*). Down the slope, these N34°E (at the summit) to N18°W (down the slope) ridges coalescence, thereby increasing the base width. The west-northwestern flank of these ridges is steeper than the east-southeastern flank at the summit, and down the slope gradient steepness reverses in both flanks. Further, the summit of all these ridges and its bifurcations exhibits a triangle faceted form.

In the present study area, the ridges observed to the west and southwest of Barren Island are identified as eastern and northeastern extensions of the IB, called here as 'Western Ridge' and 'South-Western Ridge' respectively (Figure 2 *b*). The Western Ridge trends 9°N–12°E and in the far southern end, the trend of this ridge

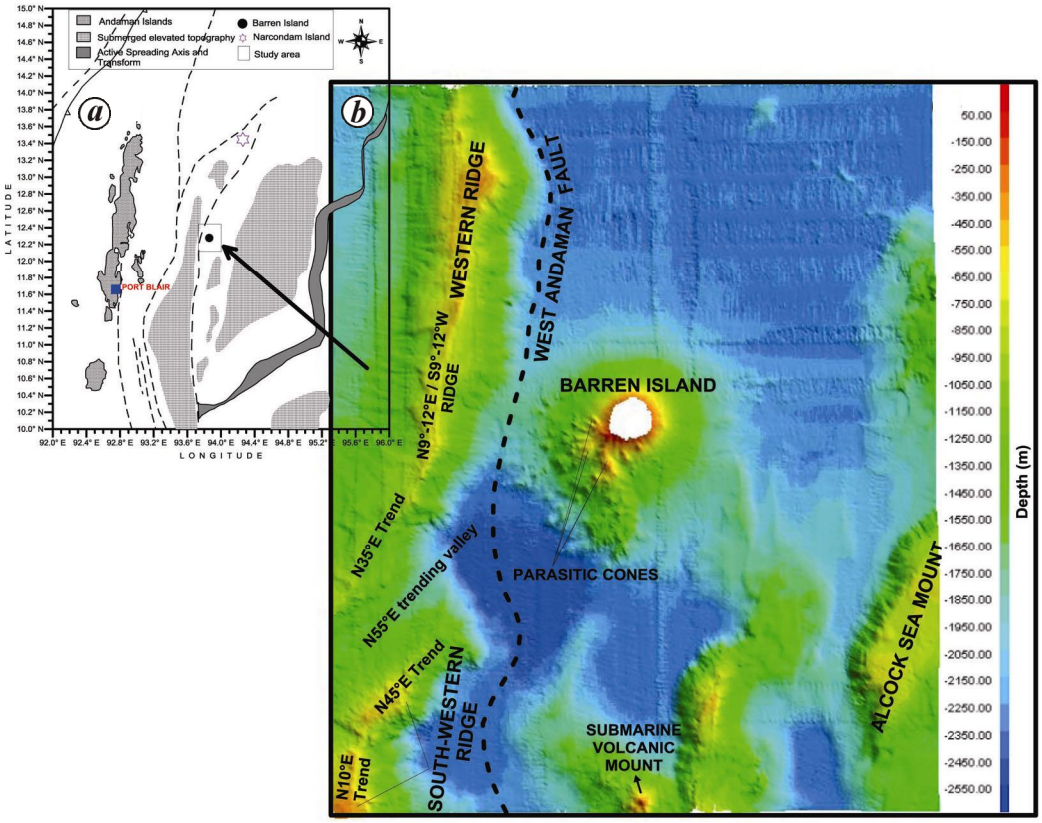


**Figure 2.** ***a***, Location map of the study area around Barren Island, Andaman Sea. ***b***, Interpreted 3D grid model of the seafloor depicting submarine geomorphic features around the Barren volcanic base.

changes to N35°E. It rises about 1104 to 1880 m above the seafloor and the width of the base of the ridge varies from 19.57 to 22.22 km, whereas the width at the peak varies from 761 to 5926 m (Figures 2 *b* and 3 *c*). The ESE (99°) sloping flank is steeper than the WNW (279°) sloping flank at the summit and becomes gentler at the base. In addition, the ESE sloping flank is characterized by the presence of submarine channels (Figures 2 *b* and 5 *a*). On the other hand, the WNW sloping flank maintains almost a constant gradient from summit to base. The 'south-western ridge' has two segments. The northern segment shows a N45°E trend and the southern segment a N10°E trend. The base of the northern portion lies 8.49 km away from the base of the BIV on the seafloor with a basal width of 14.62 km; height up to summit (located at a water depth of 761 m) from ocean floor is 1557 m (Figure 3 *b*). A N55°E trending valley which separates these ridges, located to the west of the Barren Island, is 10.12 km wide and 759 m deep. From the 3D grid model generated, it is evident that the recent flows extended up to the base of the IB.

In the study area, the northern extension of the Alcock seamount is located around 30.46 km away from the summit of the Barren Island in S59°E direction. The Alcock seamount is manifested in the form of isolated ridges (three within the study area) trending in NNE–SSW direction with flat submarine plateau top. On the southern side, the basal width of Alcock seamount varies from 6466 to 10,366 m as it rises from water depth 2297 to 1389 m. A N30°E trending ridge of Alcock seamount with flat plateau summit can be seen in the SSE direction. The configuration of Alcock seamount reveals that its southern and western flanks are steeper than those of the northern and eastern flanks (Figure 3 *c*). In the western margin of Alcock seamount, runnels and incisions are noticed.

A submarine volcanic mount has been observed 38 km south of Barren Island at 2274 m water depth (Figures 2 *b* and 3 *a*). It is a steep mount scaling to 1712 m height with its summit at 238 m water depth (Figure 3 *a*). The gradient of its flank from the summit to the base is steeper on the northern side and varies from 24.64° to 29.7° in all other directions. Its base radius varies from 3.95 to 8.77 km and its base circumference ranges from 24.78 to 55.13 km.

In the geomorphologic context, previous studies[7–9] described BIV as a roughly circular island with a diameter of ~3.2 km, without giving much information about the undersea nature of the Island. The present study shows that the base of BIV island is located at a

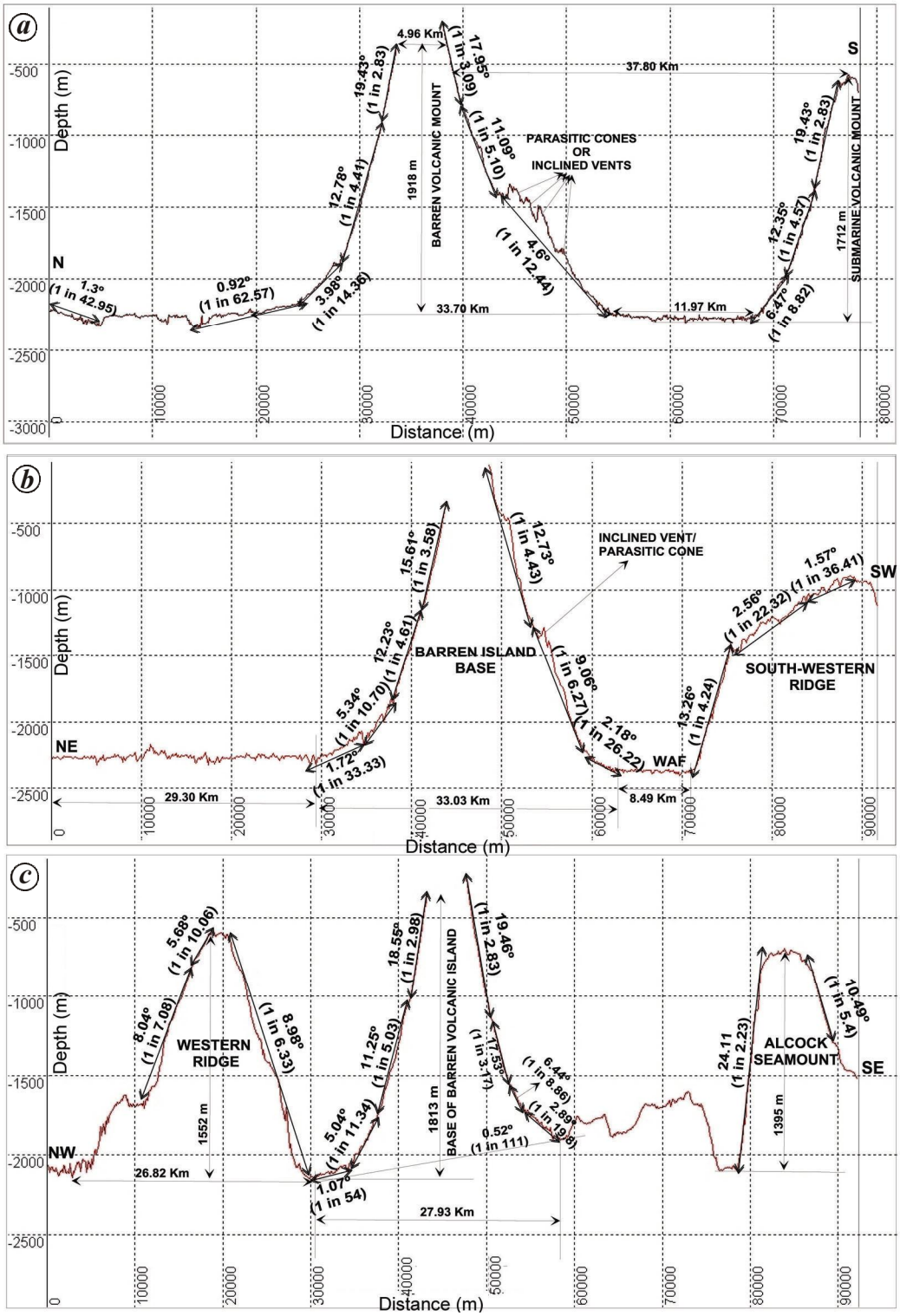


**Figure 3.** Bathymetric profile along N–S direction (***a***), NE–SW direction (***b***) and NW–SE direction (***c***) across the Barren Island.

maximum depth of ~2400 m with a maximum diameter of 36 km in the N–S direction. Three-dimensional grid model of the region shows that a large part of the volcano is submarine, suggesting much of the eruptive history of the volcano is submarine in nature. A few small mounts on the western, southwestern and southern submarine slope of the BIV island are formed as parasitic cones associated with the recent volcanic eruptions. These parasitic cones are apparently the sites for submarine volcanic eruptions, which are completely absent in the eastern and

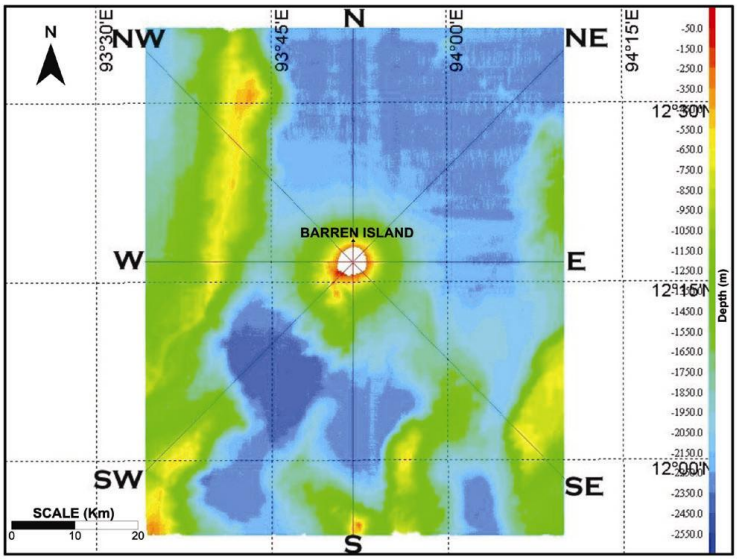


**Figure 4.** Two-dimensional grid model of the survey area with positions of the N–S, NE–SW and NW–SE profile lines.

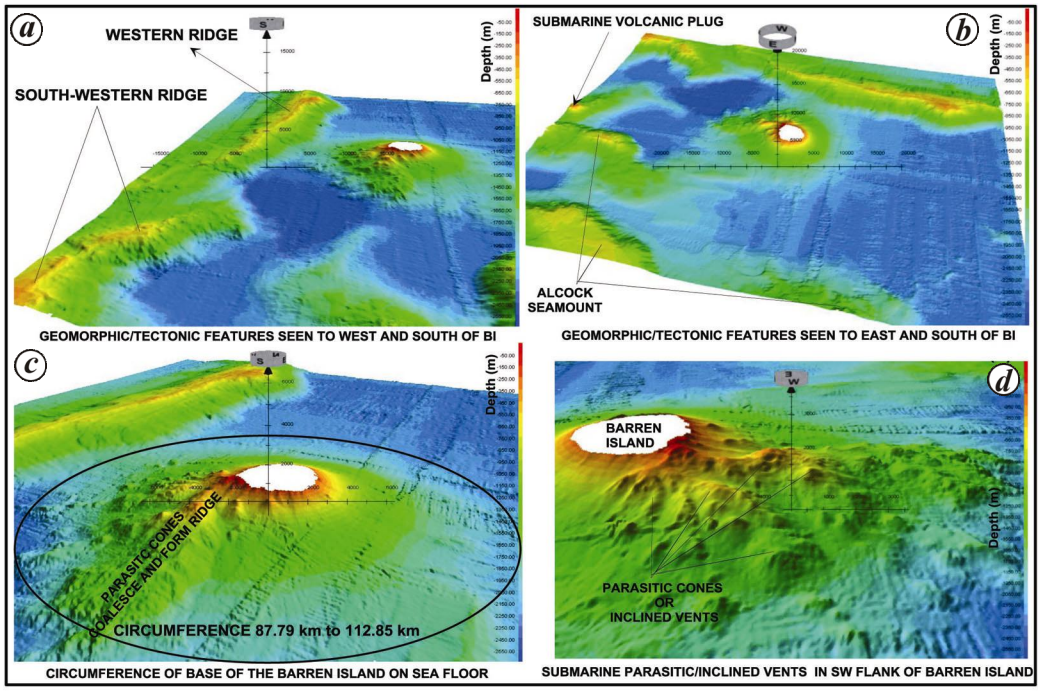


**Figure 5.** Different views of the Barren Island base and other tectonic features around Barren Island: ***a***, Eastern and northeastern extension of Invisible Bank; ***b***, Submarine volcanic plug and Alcock seamount; ***c***, Ridge formed by parasitic cones; ***d***, Numerous parasitic cones.

northern flanks. Furthermore, because of the presence of these recent submarine volcanic activities along the western and southwestern slopes[10], base of BI is extended more in these directions and the slope is considerably decreased along recent flow direction, as is evident from the profile studies. In addition, much farther dispersed submarine volcanic activities have led to the development of gentler slopes at the base of BI, which otherwise is characterized by steeper ENE flank. Although it is identified that the eruptive style of the volcano was primarily of Strombolian type, such an extension even up to the base of the IB suggests a Plinian type of eruption under the sea[11]. Sheth *et al.*[9] described the BIV flows as significantly cooled, highly crystallized and viscous with low pace of movement and continuous supply of lava. Hence, the extension of such slow-moving flows up to the base

of the Barren Island indicates large feeder systems such as the parasitic cones and continuous supply of lava from these parasitic cones below the sea during the recent eruptions. Furthermore, the abrupt fall on the eastern side of the IB is explained by the presence of WAF. A newly identified submarine mount, south of the BI, is associated with the volcanic arc in the Andaman Sea. In addition, the close relationship of the newly identified submarine volcanic mount and BIV is established, because of its proximity to the parasitic cones. Hence, the parasitic cones on the southwestern and southern submarine slopes and the submarine volcanic mounts are developed in association with the recent eruptions in 2005 and 2009. Unlike BIV island, other associated morphotectonic elements in the present study area, viz. IB and Alcock seamount are flat-topped. Furthermore, the slopes facing the Barren Island are characterized by submarine slides, which are completely absent on the other slopes. Although detailed studies are required to constrain the reasons for explaining the presence of submarine slides, it is possible that they may be related to the recent eruptions.

The present study revealed the changes in the configuration of the base of BIV. Effects of recent flows on BIV under the sea are deciphered in the form of thick flows along the western and southwestern slope, extending even up to the base of IB. Furthermore, development of parasitic cones and a newly identified submarine volcanic mount in the present study area also indicate the submarine volcanic activities associated with BIV. Development of numerous feeding sites as expressed in the form of parasitic cones provided huge volume of lava, which in turn pushed the flows to the base of IB. These recent flows reduce the steepness of BIV in the western slopes. This implies that the morphology of the Barren volcanic base is largely modified by the recent eruptions. Furthermore, it is also noteworthy that other morphotectonic elements surrounding the Barren Volcano, viz. Alcock seamount and IB are flat-topped, stable features unlike the BIV.


1. Curray, J. R., Moore, D. G., Lawyer, I. A., Emmel, F. J., Rain, R. W. and Kiecklefer, R., Geological and geophysical investigations of continental margin. *AAPG Mem.*, 1979, **29**, 189–198.
2. Curray, J. R., Tectonics and history of the Andaman Sea region. *J. Asian Earth Sci.*, 2005, **25**, 187–232.
3. Pal, T. *et al.*, The 2005–2006 eruption of the Barren Volcano, Andaman Sea: evolution of basaltic magmatism in island arc setting of Andaman–Java subduction complex. *J. Asian Earth Sci.*, 2010, **39**, 12–23.
4. Roy, T. K. and Chopra, N. N., Wrench faulting in Andaman forearc basin, India. In Proceedings Offshore Technology Conference, Houston, Texas, 1987, vol. 19, pp. 393–404.
5. Curray, J. R., Geological history of the Bengal geosyncline. *J. Assoc. Expl. Geophys*., 1991, **XII**, 209–219.
6. Ware, C. *et al.*, A system for cleaning high volume bathymetry. *Int. Hydrogr. Rev.*, 1992, **XIX**(2), 77–94.
7. Awasthi, N. *et al.*, Major ash eruptions of Barren Island volcano (Andaman Sea) during the past 72 Kyr: clues from a sediment core record. *Bull. Volcanol*., 2010, **72**, 1131–1136.
8. Sheth, H. C., Ray, J. S., Bhutani, R., Kumar, A. and Awasthi, N., The latest (2008–09) eruption of Barren Island volcano, and some thoughts on its hazards, logistics and geotourism aspects. *Curr. Sci.*, 2010, **98**, 620–626.
9. Sheth, H. C., Ray, J. S., Kumar, A., Bhutani, R. and Awasthi, N., Toothpaste lava from the Barren Island volcano (Andaman Sea). *J. Volcanol. Geotherm. Res.*, 2011, **202**, 73–82.
10. Luhr, J. F. and Haldar, D., Barren Island volcano (NE Indian Ocean): island-arc high alumina basalts produced by troctolite contamination. *J. Volcanol. Geotherm. Res*., 2006, **149**, 177–212.
11. Sheth, H. C., Ray, J. S., Bhutani, R., Kumar, A. and Smitha, R. S., Volcanology and eruptive styles of Barren Island: an active mafic stratovolcano in the Andaman Sea, NE Indian Ocean. *Bull. Volcanol*., 2009, **71**, 1021–1039.


ACKNOWLEDGEMENTS. We thank our colleagues on the cruise SM-220 and especially the Chief Scientist under whose supervision the cruise was undertaken. We also thank the Deputy Director General, Eastern Region, Geological Survey of India (GSI), Kolkata for financial assistance and the Director General, GSI, Kolkata for permission to publish this work. Processing facility for multibeam data provided by the OPEC-I, M&CSD, GSI, Kolkata is acknowledged.

Received 3 May 2014; revised accepted 27 October 2014

# Comparative study of soil profiles developed on metavolcanic (basaltic) rocks in two different watersheds of Garhwal Himalaya

**S. Vyshnavi[1], R. Islam[1,*] and Y. P. Sundriyal[2]**

[1]Wadia Institute of Himalayan Geology, Dehradun 248 001, India
[2]H.N.B. Garhwal University (Srinagar), Srinagar 246 174, India

**Soil profiles are rarely preserved in the Himalaya due to active tectonics and erosion. We have studied two rarely well-preserved soil profiles developed on metavolcanic rocks namely Alaknanda soil profile (ASP) and Bhilangna soil profile (BSP) in Alaknanda and Bhilangna watersheds of the Garhwal Himalaya. Geochemical studies were carried out to understand the elemental mobility with reference to the least altered rock (LAR) in both the profiles and are compared. Differences in major element behaviour noticed are depletion of Ca and K in ASP, and depletion of Ca and Na in BSP. Trace elements also show variable mobility such as leaching of Rb, U and enrichment of Sr, Ni in ASP. In BSP, behaviour of these elements is just the opposite. Accumulation of ∑REEs in saprolitic layer and depletion in regolith of ASP suggest that rare earth element (REE) mobility took place during advanced stages of weathering. In BSP, increase in REE content from LAR to regolith suggests**

*For correspondence. (e-mail: rislam@wihg.res.in)